Human CST complex protects stalled replication forks by directly blocking MRE11 degradation of nascent-strand DNA

Lyu et al.

Appendix Table of contents

Lyu et al. Appendix Figure S1 (continued on the next page)

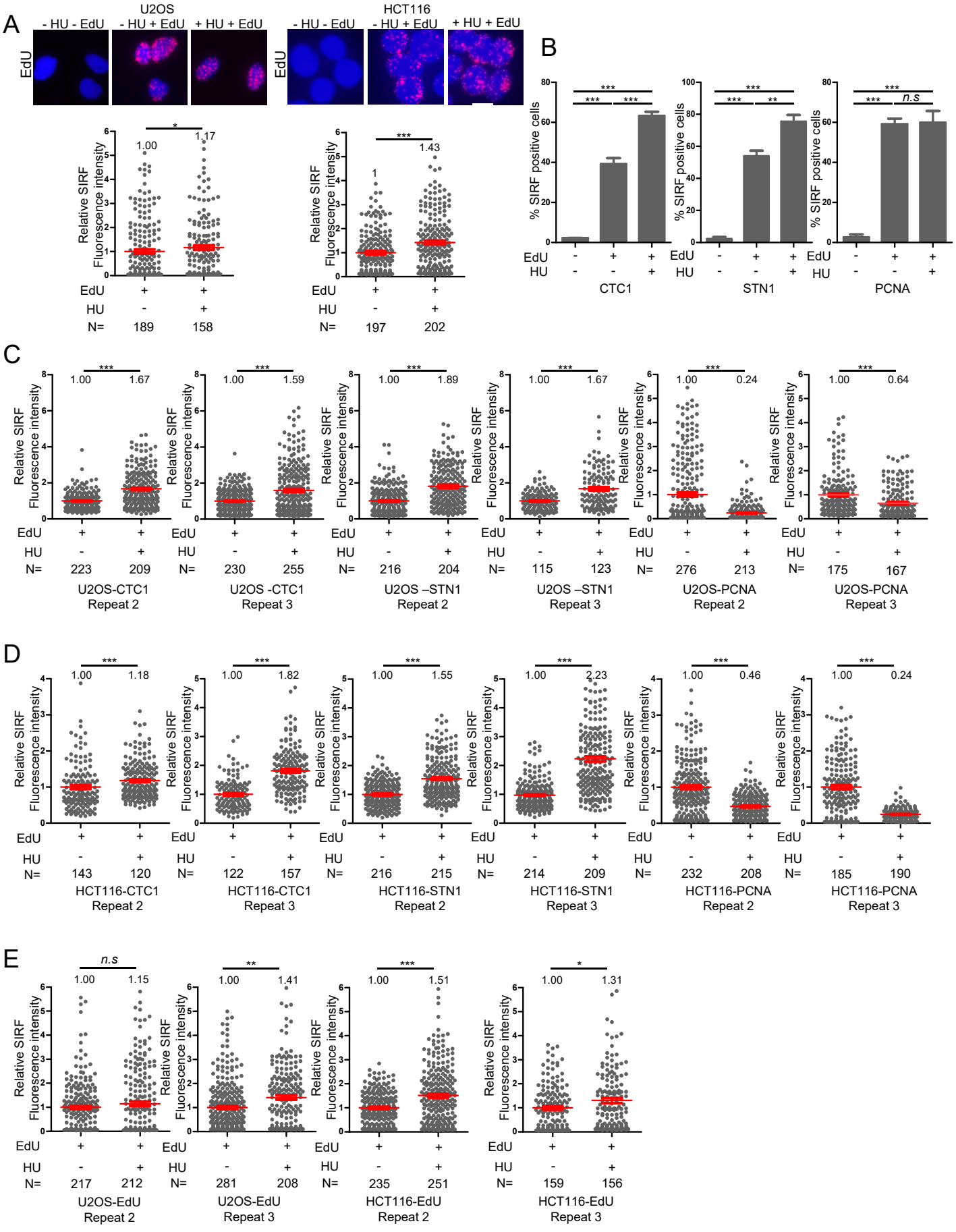

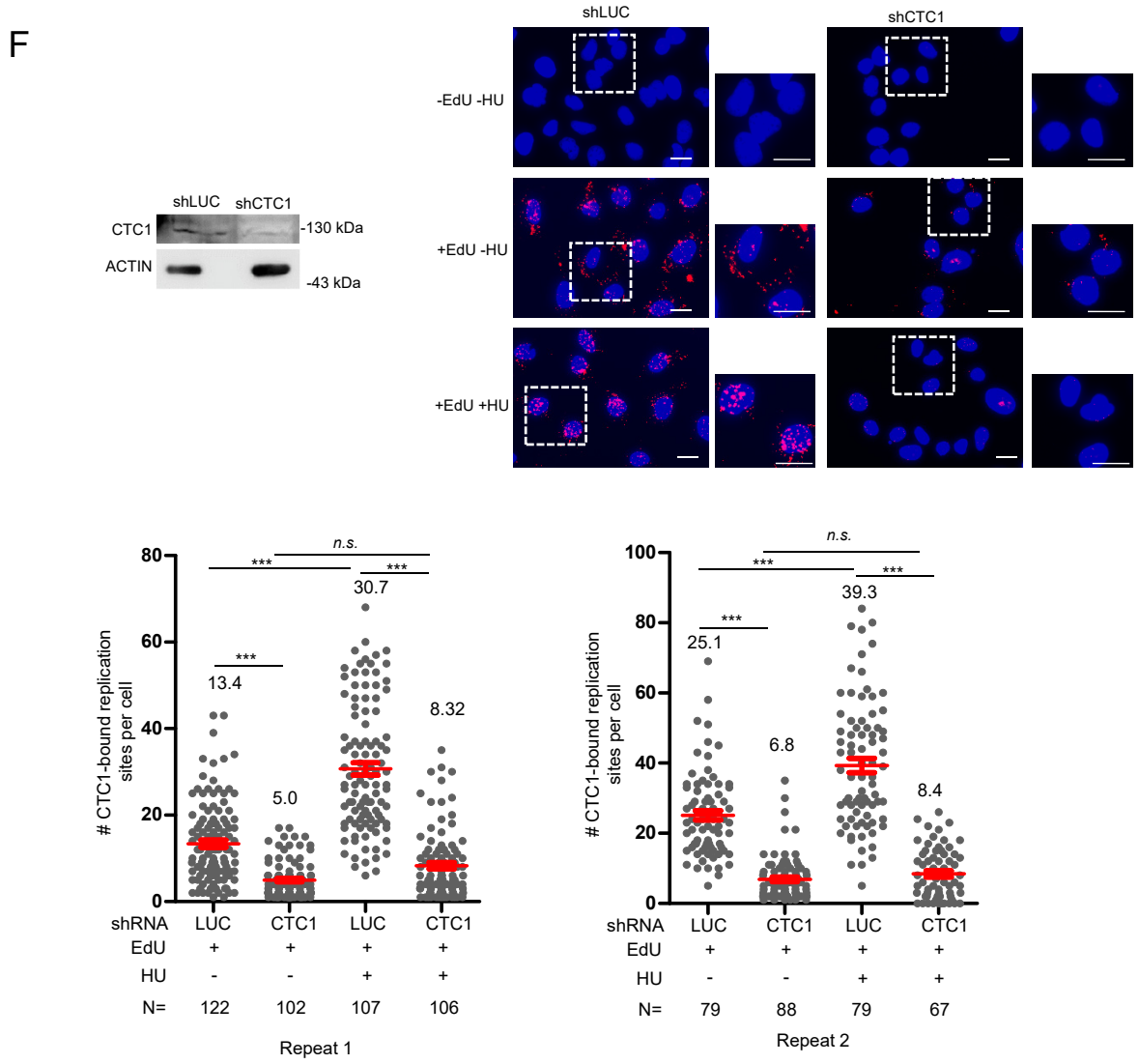

Appendix Figure S1 (Related to Figure 1). CST localizes at stalled forks. (A) EdU SIRF assay in U2OS and HCT116 cells. (B) Frequency of CTC1 SIRF (>3 foci) and STN1 SIRF (>5 foci) positive cells in U2OS cells. Statistical analyses were performed using one-way ANOVA analysis with post hoc Tukey from three independent experiments. Error bar: SEM. (C) Biological replicates of relative CTC1-SIRF, STN1-SIRF, and PCNA-SIRF fluorescence intensity with and without HU treatment in U2OS cells for Figure 1B. (D) Biological replicates of relative CTC1-SIRF, STN1-SIRF, and PCNA-SIRF fluorescence intensity in HCT116 cells for Figure 1C. (E) Biological replicates of relative EdU-SIRF fluorescence intensity in U2OS and HCT116 cells for Appendix Figure S1A. (F) CTC1 SIRF assay in CTC1-depleted U2OS cells. CTC1 knockdown efficiency was shown by western blot. Representative SIRF images of each sample are shown. Box areas are amplified and shown in inserts. Scale bars: 20 μm. Two biological replicates of SIRF assays were performed and quantification results are shown. N, the number of nuclei analyzed in each sample. *P* values were calculated by one-way ANOVA analysis with post hoc Tukey. *** $P<0.001$.

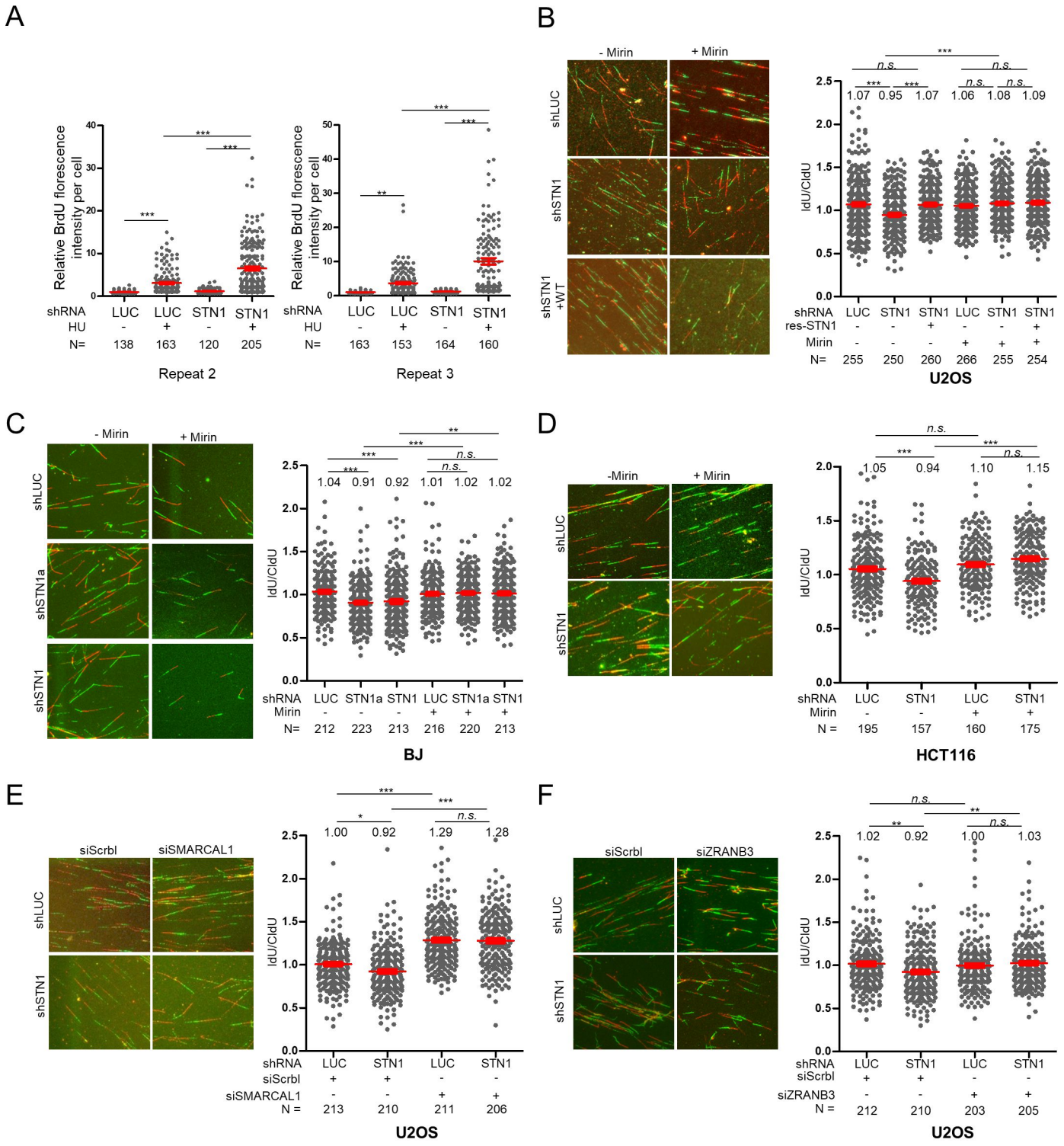

Appendix Figure S2 (Related to Figure 2). (A) Biological replicates of native BrdU fluorescence intensity for Figure 2A. (B-F) Representative images and biological replicates of DNA fiber analyses for Figure 2B-2F. *** $P<0.001$, ** $P<0.01$, * $P<0.05$.

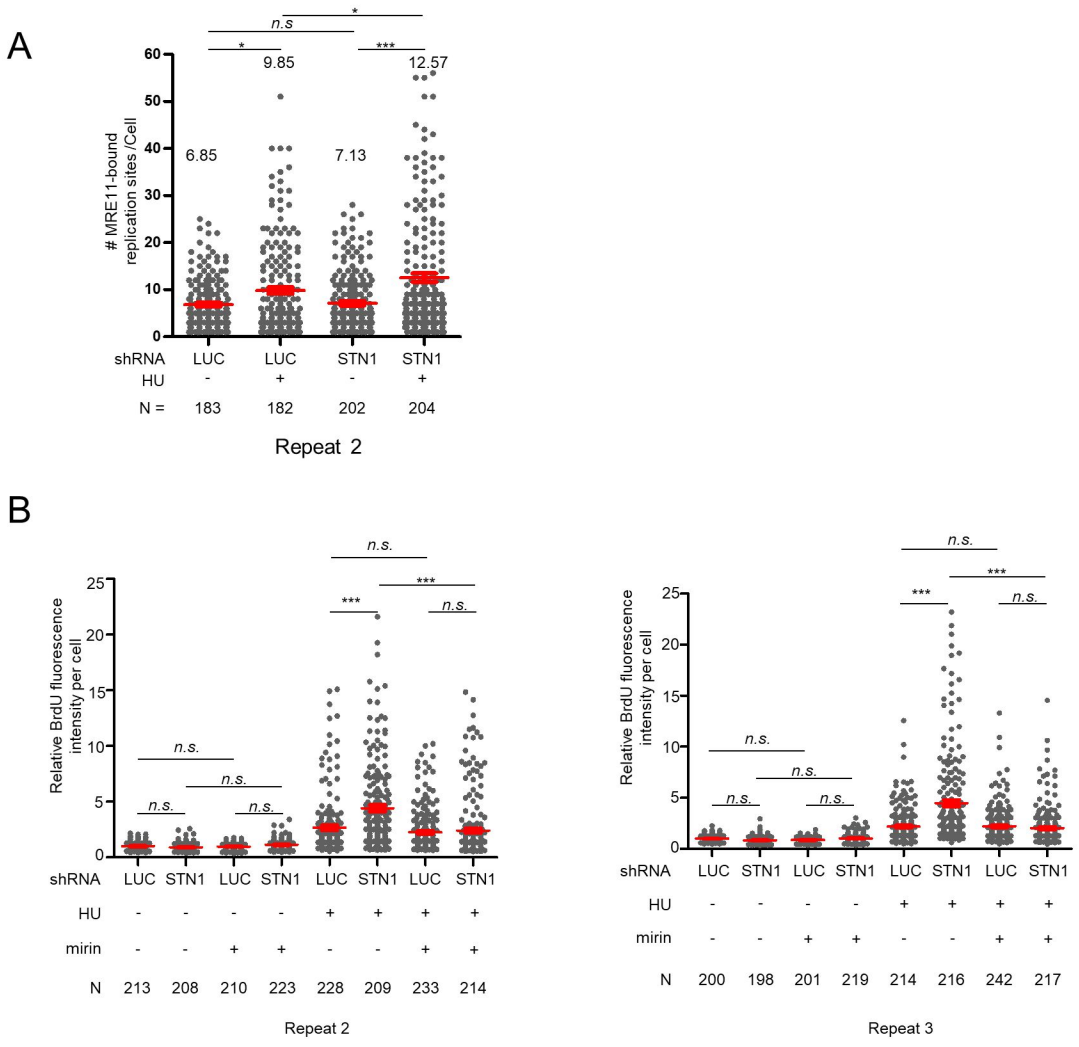

Appendix Figure S3 (Related to Figure 3). (A) Biological replicate of relative MRE11-SIRF signal foci number in U2OS for Figure 3A. (B) Biological replicates of relative native BrdU staining in shSTN1 with and without mirin treatment for Figure 3B. *** $P<0.001$, ** $P<0.01$, * $P<0.05$.

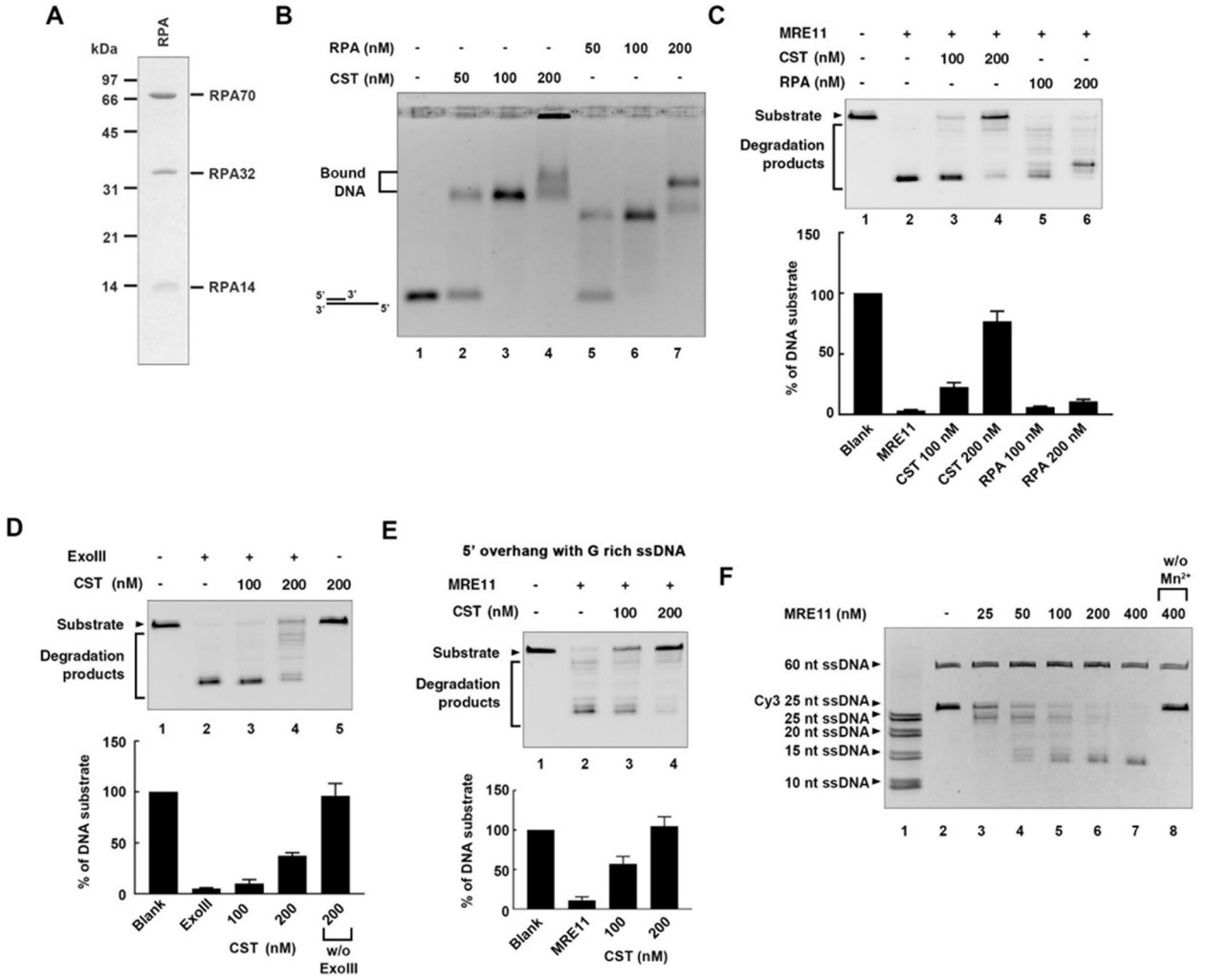

Appendix Figure S4 (Related to Figure 4). Specificity of CST against MRE11-mediated DNA degradation.

(A) Coomassie blue stained SDS-PAGE gel (15%) of purified human RPA complex.

(B) DNA binding activity of wild-type CST complex and RPA complex. The 5' Cy3-labeled substrates (80 nM) were incubated with the indicated concentrations of CST and RPA. Samples were analyzed by a 0.8% agarose gel.

(C) MRE11 degradation analysis. 5' Cy3-labeled substrates (80 nM) were pre-incubated with indicated concentrations of CST or RPA at 37°C for 5 min. Reactions were completed by adding MRE11 (400 nM) for an additional 40 min incubation and then stopped by SDS and proteinase K. Samples were resolved in a 27% denatured polyacrylamide gel. The results are graphed and error bars represent the standard deviation (± SD) calculated from at least three independent experiments.

(D) ExoIII degradation analysis. 5' Cy3-labeled substrates (80 nM) were pre-incubated with indicated concentrations of CST at 37°C for 5 min. Reactions were completed by adding ExoIII (0.01U) for an additional 20 min incubation and then stopped by SDS and proteinase K. Samples were resolved in a 27% denatured polyacrylamide gel. The results are graphed and error bars represent the standard deviation (± SD) calculated from at least three independent experiments.

(E) MRE11 degradation analysis. 5' Cy3-labeled G-rich substrates (80 nM) were pre-incubated with indicated concentrations of CST complex. Reactions were completed by adding MRE11 (200 nM) for an additional 20 min incubation and then stopped by SDS and proteinase K. Samples were resolved in 27% denatured polyacrylamide gel. The results are graphed and error bars represent the standard deviation (± SD) calculated from at least three independent experiments.

(F) SYBR GOLD staining of MRE11 degradation experiment as Figure 5B with indicated length ssDNA as a reference marker.

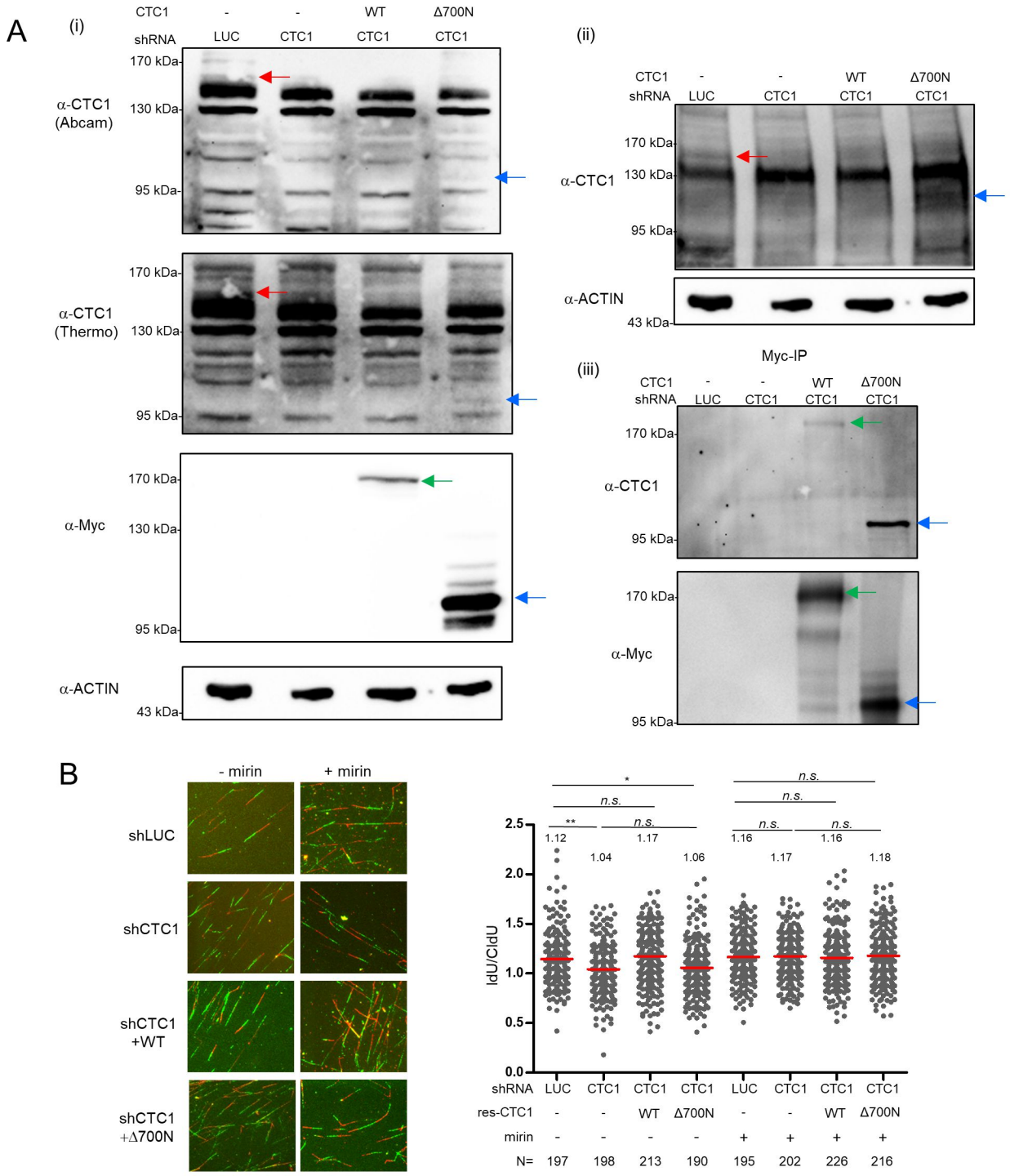

Appendix Figure S5 (Related to Figure 5). (A) Western blot showing CTC1 knockdown and co-expression of shCTC1 with RNAi-resistant Myc-CTC1-WT or Δ700N in U2OS cells. Equal amount of whole cell lysates of each sample were separated on an 8% SDS-PAGE (i) and a 4-15% gradient gel (ii). Gels were run in parallel and western was performed at the same time. Endogenous CTC1 (red arrow) was detected by two different CTC1 antibodies obtained from different vendors, ThermoFisher and Abcam. While the anti-myc antibody easily detected exogenously expressed Myc-CTC1 (green arrow) and Myc-Δ700N (blue arrow), full-length Myc-CTC1 could not be detected by the anti-CTC1 antibody, and Myc-Δ700N was weakly detected by anti-CTC1. (iii) Exogenously expressed Myc-CTC1 could be detected by anti-CTC1 only after being enriched by IP with anti-Myc antibody. Similar results were observed previously (Wang et al. 2018, Nucleic Acid Research, https://doi.org/10.1093/nar/gky114) (B) Representative DNA fiber images and quantification results from the biological replicate for Figure 4E. * P<0.05, ** P<0.01.

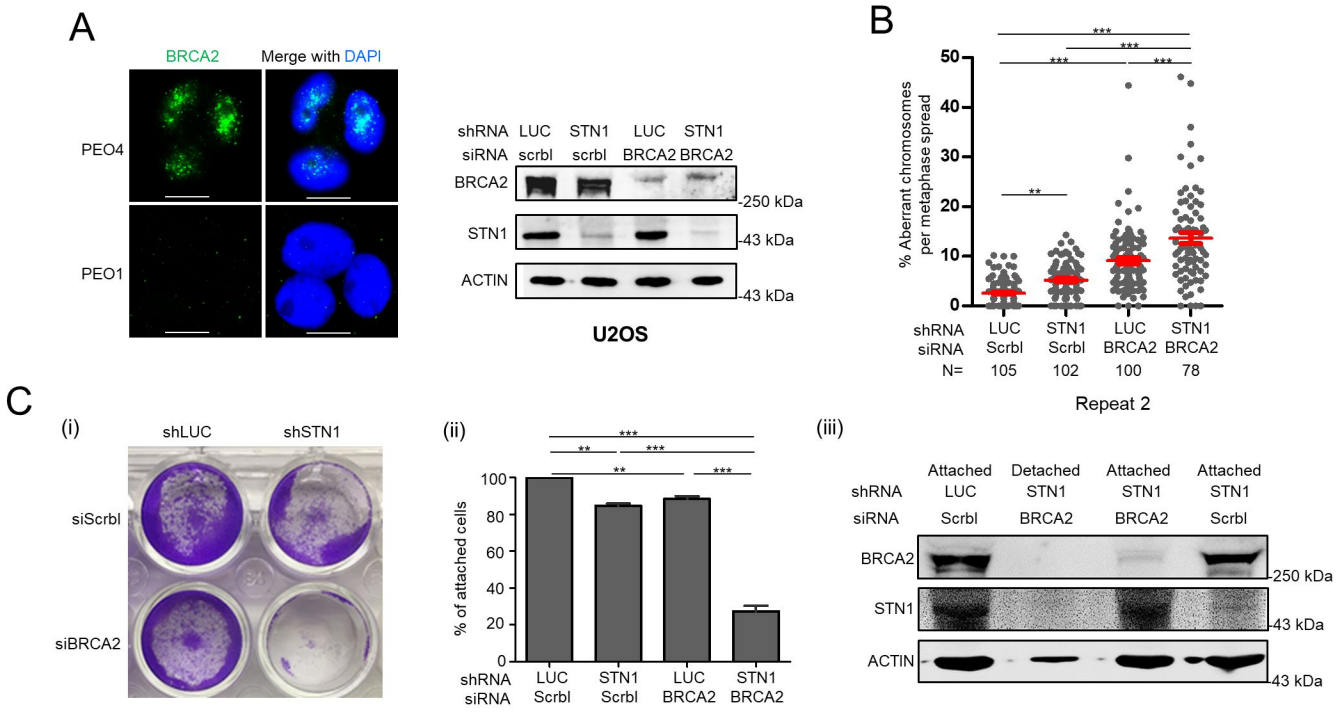

Appendix Figure S6 (Related to Figure 6). Genetic relationship of CST and BRCA2 in protecting genome stability. (A) Specificity of the BRCA2 antibody. Left: Immunofluorescence analysis using the anti-BRCA2 antibody in BRCA2-deficient (PEO1) and -proficient (PEO4) human ovarian tumor-derived cells. Right: Western blot showing the knockdown of STN1 and BRCA2 in U2OS cells. All cells were collected and subject to cell lysis and western blotting. (B) The biological replicate of aberrant chromosomes in STN1 and BRCA2 co-depleted cells upon HU treatment for Figure 6E. ***P<0.001. (C) Co-depletion of STN1 and BRCA2 in U2OS induced massive cell detachment from the dish. U2OS stably expressing shSTN1 were transfected with BRCA2 siRNA or control siRNA (scramble). (i) After transfection, detached cells were washed away and cells that remained attached to the dish were stained with crystal violet. (ii) Attached cells were collected, cell numbers were counted with trypan blue staining in a hemocytometer, and then normalized to the shLUC siScrbl control. Quantification results were from three independent experiments. P values were calculated by one-way ANOVA analysis with post hoc Tukey from three independent experiments. Error bars: SEM. ** P<0.01, *** P<0.001. (iii) Detached and attached cells were collected and cell lysates were subject to western blotting to detect BRCA2/STN1 knockdown. While STN1 depletion remained effective in single knockdown cells (last lane), STN1 expression was recovered in attached cells after BRCA2/STN1 co-depletion (second from the right lane).

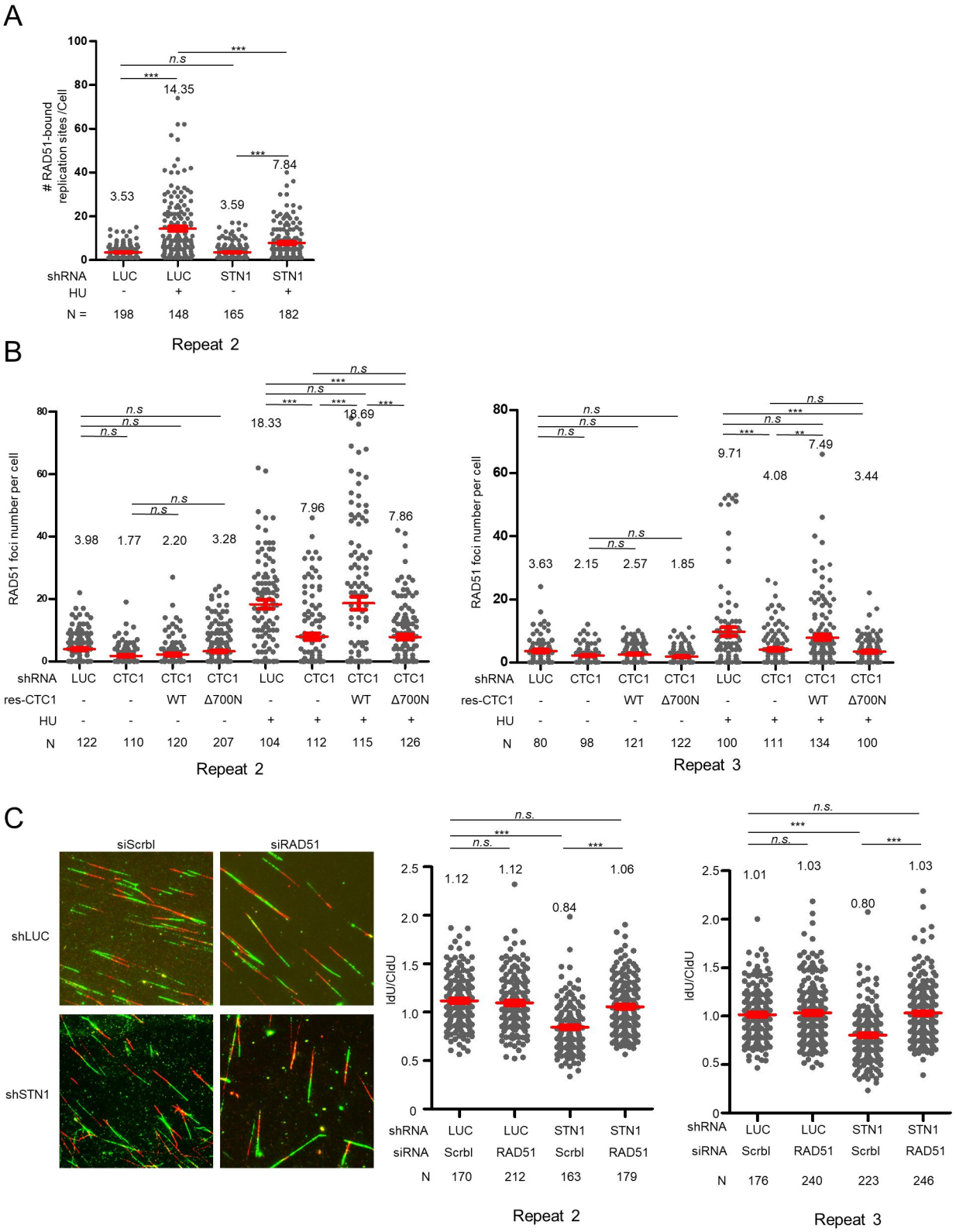

Appendix Figure S7 (Related to Figure 7). CST facilitates RAD51 recruitment to stalled replication forks. (A) The biological replicate of relative RAD51-SIRF foci number per cell for Figure 7A. (B) Biological replicates of RAD51 immunofluorescence foci number per cell for Figure 7B. (C) Representative images and biological replicates of DNA fibers for Figure 7C. *** $P<0.001$.

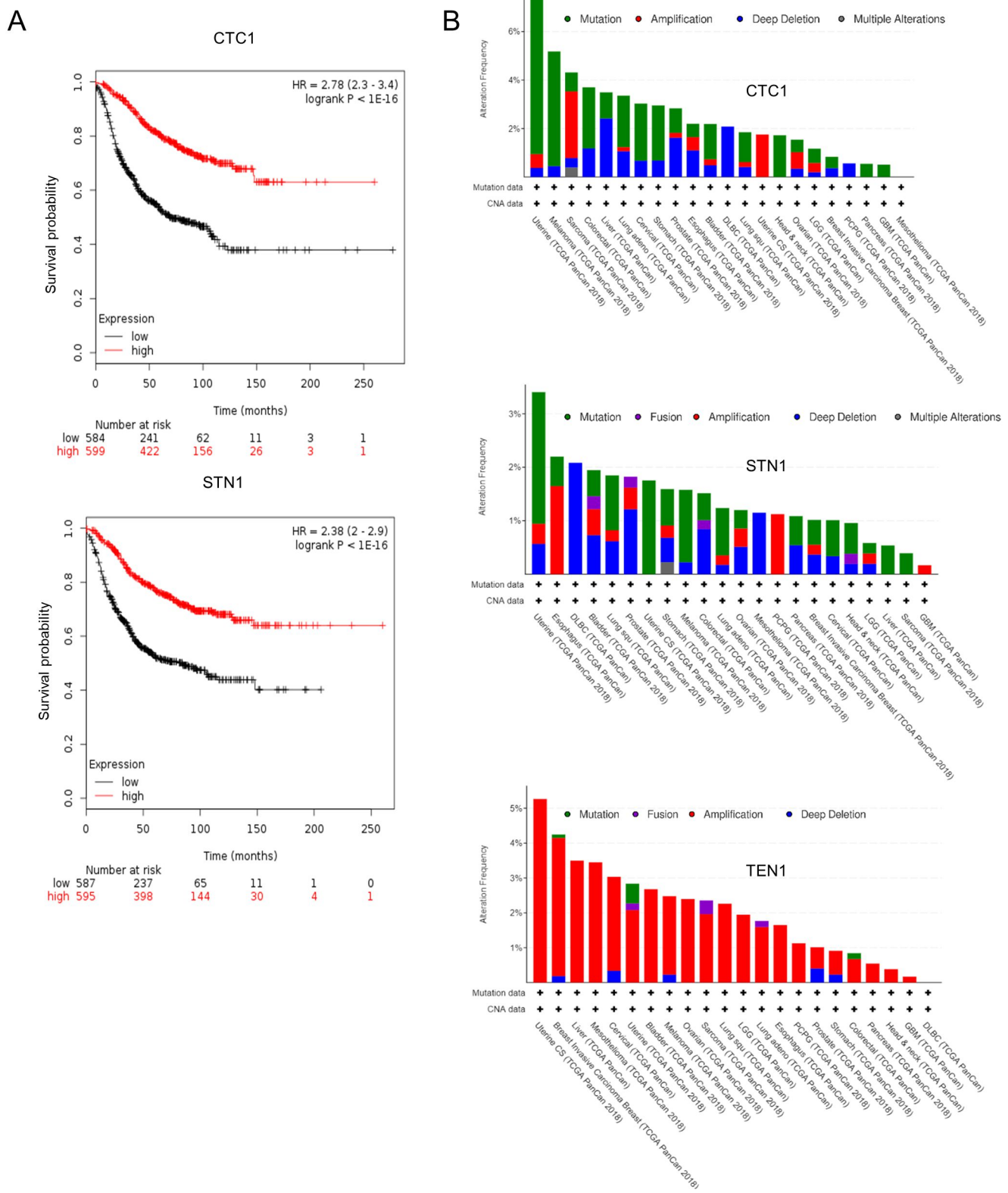

Appendix Figure S8. Clinical data analysis of CST. (A) Kaplan-Meier analysis shows overall survival probability of breast cancer patients separated based on CTC1 and STN1 expression at upper tertile and lower tertile level. Plots are shown as percent survival (survival probability). Red lines indicate the survival of patients with the upper tertile of CTC1/STN1 expression level, while black lines indicate the survival of patients with the lower tertile of CTC1/STN1 expression level. Numbers below the plots are number of patients included in analysis in each group. (B) CST gene alteration frequency in different types of tumors. Data are derived from TCGA PanCancer Atlas.